Double-period zero-order metal gratings as effective selective absorbers

W.-C. Tan, J. R. Sambles, and T. W. Preist
Thin Film Photonics Group, School of Physics, University of Exeter, Stocker Road, Exeter EX4 4QL, United Kingdom
(Received 21 September 1999; revised manuscript received 16 December 1999)

The electromagnetic response of a zero-order metal grating having a primary deep short-period component and a shallow long-period component is modeled. It is found that such a metal grating has an unusual surface-plasmon-polariton band structure and exhibits strong selective absorption of incident radiation. This opens up potential for designing metal surfaces with specific optical response features.

I. INTRODUCTION

A surface plasmon polariton (SPP) is an excitation localized on a metal-dielectric interface, which is a composite of an electromagnetic wave in the dielectric and a surface plasma wave, a collective electronic excitation, in the metal.[1] On a flat metal surface, an SPP mode can not be directly coupled to by incident radiation because the dispersion curve of the SPP is beyond the light cone (the in-plane momentum of the SPP is greater than the maximum available photon momentum in the adjacent dielectric). When a grating is created on a metal surface, two closely related physical effects occur. First, the periodicity of the grating provides additional in-plane momentum for the incident photons, which enables the excitation of the surface-plasmon-polariton by electromagnetic radiation. This mechanism, often called ''grating coupling,'' has long been used to study the SPP modes on metal surfaces. Second, the grating also splits the SPP dispersion curve into bands, just as the electron states in a periodic potential form into bands. As we will discuss, these two effects open the opportunity for designing the optical properties of metal surfaces by choosing suitable grating profiles.

Here we consider a simple double-period grating described by

$$z = A_1 \sin\left(\frac{2\pi}{l}x\right) + A_n \sin\left(\frac{2\pi}{nl}x + \alpha_n\right), \qquad (1)$$

where n is an integer greater than one. The first term on the right side of Eq. (1) is the principal component of the grating which has an amplitude of A_1 and a period of l. The second term has an amplitude of A_n ($\ll A_1$), a period of nl ($n \geqslant 2$), and a relative phase of α_n. We are particularly interested in the case where the grating is zero order, i.e., $\lambda > 2nl$, where λ is the electromagnetic wavelength.

To appreciate the electromagnetic properties of the double-period grating, we first consider the case of $A_n = 0$, $n \neq 1$, i.e., a sinusoidal zero order grating. It is known from previous studies that very flat SPP bands may be formed on a deep short pitch metal grating,[2,3] each band corresponding to a standing SPP mode localized in the grating grooves.[3–6] However, within the light cone, the SPP modes on such a sinusoidal grating are very broad (or short ranged) because they are strongly radiative.[3] Consequently, the excitation of the SPP modes only leads to weak absorption of the incident light over a rather wide range of the frequency band, i.e., a deep zero-order single-period sinusoidal grating does not drastically change the optical properties of the metal surface except for the case of a large incident angle where sharp resonant absorption may occur. Now let us consider the case in which A_2 takes a small (compared to A_1) but nonzero value. Since $A_2 \ll A_1$, the large period component will not significantly change the SPP dispersion except for band-folding effects (note that the size of the Brillouin zone, π/l, is now only half of the original size, $2\pi/l$). However, such a weak long-period component has a drastic effect on the electromagnetic response of the metal surface. This is because the originally nonradiative long-range SPP modes near the original Brillouin zone boundary ($k \approx \pi/l$) are now folded into the light cone, and thus they can now be excited by incident radiation leading to strong resonant absorption. (A slightly different way of saying this is that the weak long-period component provides extra in-plane momentum, in multiples of π/l, for the incident photons, and therefore allows direct coupling between the incident radiation and the long range SPP modes created by the principal deep grating.)

Note that the frequencies of the standing-wave SPP modes in the grooves are determined by the deep short-period component only, whilst the strength of coupling between the incident radiation and the long range SPP is determined by the weak long-period component of the grating. Therefore, by choosing suitable parameters of the principal components (i.e., l and A_1) one can achieve any required SPP resonant frequencies, and at the same time, by choosing appropriate parameters of the weak long-period component, one can obtain any required absorption line shape.

II. METHOD

Our calculation is based on a method originally proposed by Chandezon *et al.*[7] The method has been improved and applied to study a wide range of diffractive grating systems.[8–12] Very recently, we have extended the method to calculate the photonic band structures of multilayer grating systems[13] and the SPP dispersion of metal gratings.[3,5] The essence of the method is to map the curved surface onto a flat plane by the use of a nonorthogonal curvilinear coordinate transformation. Maxwell's equations are then solved in the new coordinate system for both the top medium and the substrate. Matching the tangential components of the fields

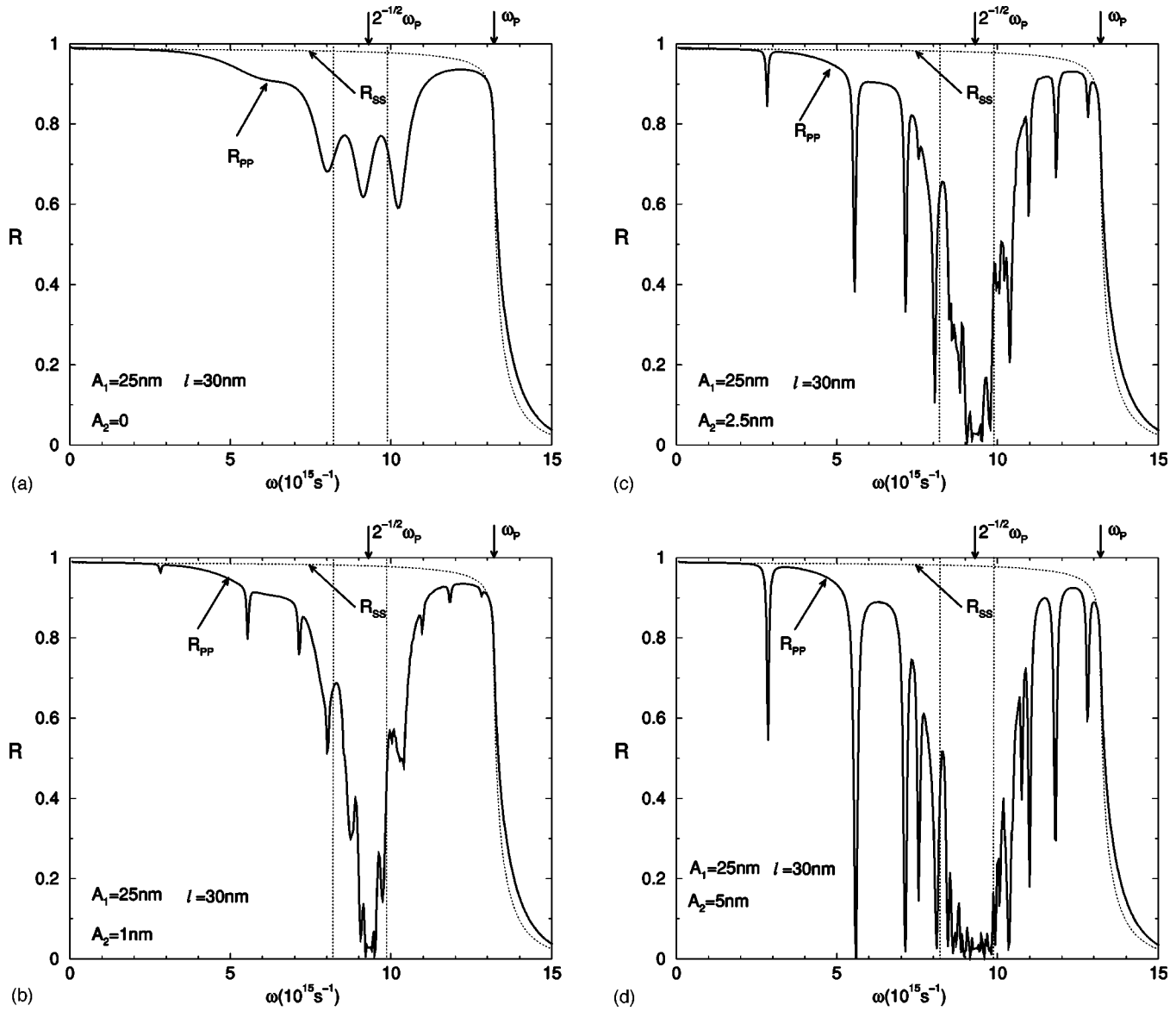

FIG. 1. The reflection coefficient as a function of frequency for normally incident radiation calculated for four double-period silver gratings described by Eq. (4), which have the same principal component ($A_1=25$ nm, $l=30$ nm), but different long-period components. (a) $A_2=0$, $\alpha_2=0$. (b) $A_2=1$ nm, $\alpha_2=0$. (c) $A_2=2.5$ nm, $\alpha_2=0$. (d) $A_2=5$ nm, $\alpha_2=0$. Note that results between the two vertical dotted lines in the vicinity of $\omega_p/\sqrt{2}$ are not numerically convergent for the reasons given in the text.

across the interface, we calculate the scattering matrix of the interface defined by

$$\begin{pmatrix} \mathbf{C}_T^+ \\ \mathbf{C}_S^- \end{pmatrix} = S \begin{pmatrix} \mathbf{C}_T^- \\ \mathbf{C}_S^+ \end{pmatrix}, \tag{2}$$

where $\mathbf{C}_T^+$ ($\mathbf{C}_T^-$) is a vector containing the coefficients of upward (downward) going eigenmodes in the top medium and $\mathbf{C}_S^+$ ($\mathbf{C}_S^-$) is a vector containing the coefficients of upwards (downwards) going eigenmodes in the substrate. The reflection and transmission coefficients of the grating are then calculated using the scattering matrix. Dispersion curves of the SPP's are obtained by finding the poles of the scattering matrix in the frequency–wave-vector ($\omega-\mathbf{k}$) plane.[3,5]

We assume the top medium and the substrate are air and silver, respectively. The dielectric function of the silver is described by a simple free-electron Drude model,

$$\epsilon_m(\omega)=1+\frac{i\tau\omega_p^2}{\omega(1-i\omega\tau)}, \tag{3}$$

where ω_p is the plasma frequency and τ is the relaxation time of the electrons. In our calculation we have taken $\omega_p=1.32\times10^{16}\ \mathrm{s}^{-1}$ and $\tau=1.45\times10^{-14}$ s; values for silver.[14]

III. RESULTS

In Fig. 1 we present the reflection coefficients for both TM (p) and TE (s) polarized normally incident electromagnetic waves calculated for several double-period silver gratings described by

$$z = A_1 \sin\left(\frac{2\pi}{l}x\right) + A_2 \sin\left(\frac{2\pi}{2l}x + \alpha_2\right). \tag{4}$$

In this calculation we fix $l = 30$ nm, $A_1 = 25$ nm, $\alpha_2 = 0$, while A_2 is taken to be 0, 1, 2.5, and 5 nm for the four gratings, respectively. (Calculations were also performed for grating profile with different nonzero values of α_2. It is found that, for the case of $A_2 \ll A_1$, the electromagnetic response of the grating is not very sensitive to α_2. Therefore, we only present here the results obtained with $\alpha_2 = 0$.) In our notation, a normally incident TM (TE) wave has its magnetic field (electric field) in the direction perpendicular to the grating vector.

Figure 1 shows that the reflection coefficient curves for TE polarized waves, incident in a plane containing the grating vector, are almost independent of the detailed profiles of the zero-order gratings. For $\omega < \omega_p$, a TE polarized incident wave is nearly totally reflected. This is because TE polarized electromagnetic waves cannot excite SPP's for this geometry, and therefore there is no strong absorption mechanism. Since the gratings are zero order, there are no diffracted orders. As a result, the reflection coefficient is not sensitive to the detailed grating profile. For $\omega > \omega_p$, both the TE and the TM polarized incident waves can excite bulk plasmons in the metal, resulting in strong absorption, so that the reflection coefficient becomes very small.

In contrast to the TE polarized waves, a TM polarized wave, incident in a plane containing the grating vector, can excite the SPP's on the grating surface, and its reflection coefficient may be very sensitive to the grating profile. Figure 1(a) shows that, for the case $A_2 = 0$, which represents a pure sinusoidal grating, the reflection coefficient is significantly different from unity only in the vicinity of $\omega_p/\sqrt{2}$, the surface-plasmon frequency of a flat surface, and in the region $\omega > \omega_p$, where bulk plasmons are excited. However, when a weak long-period (60 nm) component is introduced into the grating, very narrow but deep reflection minima appear in the frequency regions where previously the radiation would be nearly totally reflected by the original single-period grating. Since the gratings are zero order in the whole frequency region considered here, there is no higher order diffraction, therefore any deviation from total reflection is due to absorption. Figures 1(a)–1(d) illustrate that even when the amplitude of the long-period component is small compared to that of the principal component, the effect on the optical response of the silver grating is dramatic.

The physical mechanism of this effect is best understood by examining the SPP band structures. We have calculated the SPP dispersion curves of the single period grating (with $l = 30$ nm and $A_1 = 25$ nm) as well as those of a double-period grating (with $l = 30$ nm, $A_1 = 25$ nm, $A_2 = 2.5$ nm and $\alpha_2 = 0$). Figure 2(a) shows the SPP dispersion curves of the single period sinusoidal silver grating. It can be seen that quite flat bands are formed in the frequency regions both below and above $\omega_p/\sqrt{2}$. Such flat-band features of the short-pitch metal gratings were first found by Laks, Mills, and Maradudin[2] in the early 1980's using an integral method proposed by Toigo *et al.*[15] Only recently, however, has a clear physical picture for the formation of such flat surface-plasmon bands been proposed by the present authors.[3,5] It is now understood that the flat bands below $\omega_p/\sqrt{2}$ originate

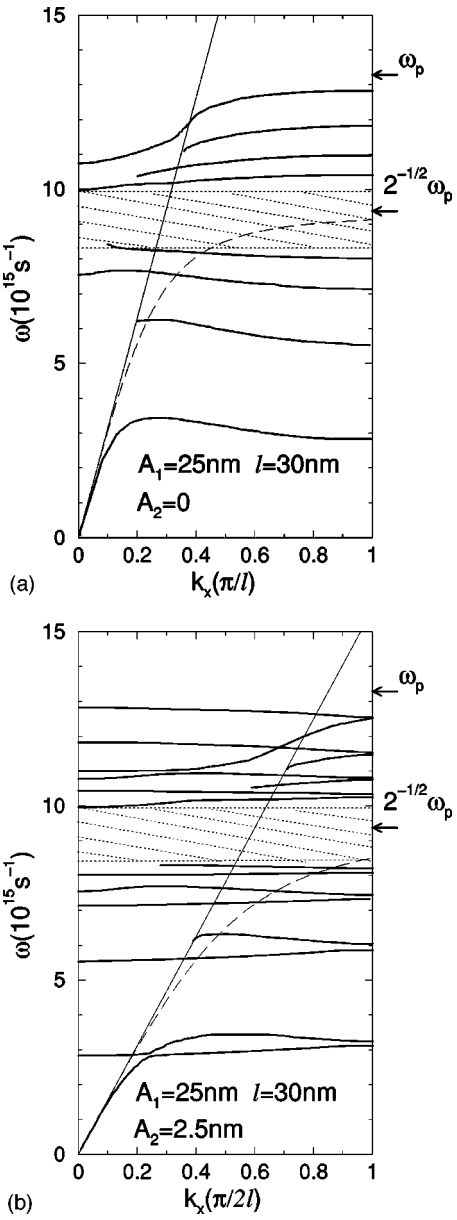

FIG. 2. The calculated SPP dispersion relations (thick solid lines) for two zero-order silver gratings. (a) A pure sinusoidal grating with $A_1 = 25$ nm, and $l = 30$ nm. (b) A double-period grating with $A_1 = 25$ nm, $l = 30$ nm, $A_2 = 2.5$ nm, and $\alpha_2 = 0$. Also plotted are the light line (thin solid lines) and the SPP dispersion on a flat silver/air surface (dotted lines). The shaded area indicates the region where convergent results have not been obtained for the reasons described in the text.

from coupled surface plasmon modes strongly localized in the grating grooves,[5] while those above $\omega_p/\sqrt{2}$ are derived from surface plasmon modes localized at the peaks of the metal surfaces.[3] Since the dispersion curve of the surface plasmon on a flat surface at $\omega = \omega_p/\sqrt{2}$ is flat, a periodic modulation of the surface will create effectively an infinite number of bands due to band folding. Consequently, the separation between bands in the vicinity of $\omega_p/\sqrt{2}$ is very small, and it is very difficult to resolve them in numerical calculations. A feature of Fig. 2(a) is that, apart from within close proximity of $\omega_p/\sqrt{2}$, the SPP modes within the light cone are very broad due to the strong radiative damping and

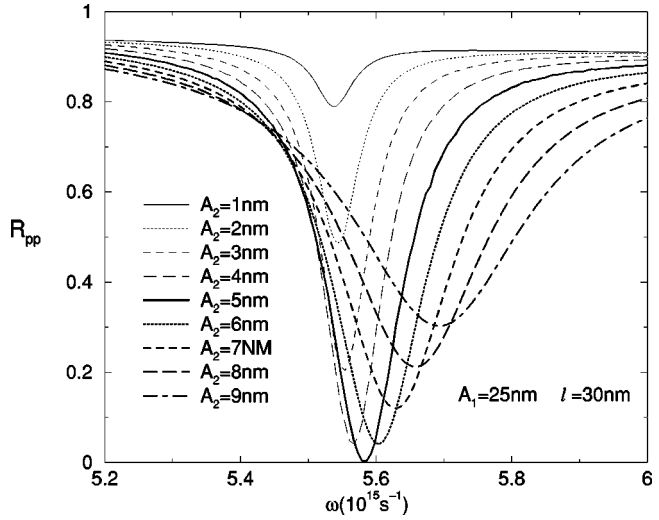

FIG. 3. Reflection coefficients near the second SPP resonance for TM polarized normally incident radiation from a series of double-period silver gratings containing the same principal component ($A_1=25$ nm, $l=30$ nm), but with different amplitudes for the long-period components (A_2) and $\alpha_2=0$.

therefore give no significant resonances in the scattering matrix. As mentioned earlier, such strong radiative damping of the SPP modes within the light cone is common for pure sinusoidal gratings.

Figure 2(b) shows the SPP band structure of the double-period grating (with $A_1=25$ nm, $l=30$ nm, $A_2=2.5$ nm, $\alpha_2=0$). Since the repeat unit of the double-period grating is twice that of the principal component, the size of the new Brillouin zone is half the original. Thus Fig. 2(b) can be easily understood by use of the zone folding scheme. There are two important differences between Figs. 2(a) and 2(b). First a small band gap opens at $k=\pi/2l$ in each SPP band of the original deep short pitch grating due to the perturbation introduced by the long-period ($2l$) component. Second, the originally nonradiative modes at $k=\pi/l$ of the pure sinusoidal grating are now folded to the Brillouin zone center, $k=0$, and hence become radiative. These modes become radiative only because of the existence of the long-period components of the grating, therefore their radiative broadening, $\Delta\omega_{rad}$, is small as long as A_2 is small. When the normally incident TM polarized EM wave matches the frequency of one of these modes, sharp resonant absorption occurs; the first five minima in Fig. 1(c) occur at frequencies which agree with the frequencies determined by the intercepts of the first five bands in Fig. 2(b) with the $k_x=0$ axis.

Since the radiative broadening of such a SPP mode is determined by the long period component of the grating, one can easily change $\Delta\omega_{rad}$ by adjusting A_2. This is illustrated in Fig. 3 where we plot the reflection coefficients for normally incident TM polarized radiation near the second SPP resonance calculated with a fixed $A_1=25$ nm and various values of A_2.

These numerical results show the optical response of the grating as the amplitude of the long period component is increased and they show the interesting feature that one can find an optimum value of A_2 that yields total absorption. This feature can be understood using a simple phenomenological model based upon the Breit-Wigner formula of multichannel resonance theory.[16] Without the SPP, the grating is effectively highly reflective and $R_0\approx 1$, because the grating is zero order. Once the A_2 component is present, an absorption channel is open via SPP radiation. This can be described in the first approximation by a two channel model in which the SPP can lose energy by radiation (width $\Delta\omega_{rad}$) and by thermal heating loss to the metal (width $\Delta\omega_{therm}$).

Within the two channel model, the Breit-Wigner approximation gives

$$T_0\approx\frac{4\Delta\omega_{rad}\Delta\omega_{therm}}{(\omega-\omega_0)^2+(\Delta\omega_{therm}+\Delta\omega_{rad})^2}, \tag{5}$$

for the transmission coefficient into the loss channel in the region of the SPP frequency ω_0. Since this is the only energy loss mechanism, then in this region $R_0\approx 1-T_0$, and so the reflection coefficient depends critically upon the relative magnitudes of $\Delta\omega_{therm}$ and $\Delta\omega_{rad}$, which are measures of the relative probabilities of energy loss by the thermal and radiative channels. These widths depend upon the parameter of the grating and the numerical calculation enables one to model the response exactly, thereby providing a design tool for a frequency selective absorbing surface.

In the whole frequency region considered here and within the light cone, the thermal broadening of the SPP modes on a *pure sinusoidal grating* is much less than the strong radiative broadening. At a low frequency ($\omega\ll\omega_p/\sqrt{2}$), $|\epsilon_{silver}|\gg 1$, it is very difficult for the electromagnetic (EM) fields to penetrate into the metal, and therefore $\Delta\omega_{therm}$ is very small. The excitation of such an SPP mode by incident radiation only leads to a very shallow absorption, as can be seen from Fig. 1(a). As the frequency increases, the amplitude of ϵ_{silver} decreases, making it easier for the EM fields to penetrate into silver, and so the thermal broadening widths of the SPP modes increase. Consequently, SPP modes at higher frequencies lead to deeper absorption minima. In the vicinity of $\omega_p/\sqrt{2}$, there are so many SPP bands squeezed into a narrow frequency range that the excitation of these modes leads to very strong absorption, even though each SPP mode in this region is overcoupled, i.e., $\Delta\omega_{rad}>\Delta\omega_{therm}$. (It is very difficult to achieve numerically convergent reflection coefficients in this frequency region for the same reason as in the dispersion calculation.) In the frequency region $1.0\times 10^{16}\ \mathrm{s}^{-1}<\omega<\omega_p$, the SPP modes become very well separated again and the absorption becomes very weak. When $\omega>\omega_p$, the incident waves are nearly completely absorbed because of excitation of bulk plasmons in the silver.

Turning again to Fig. 3, it can be seen that when $A_2=1$ nm, the reflection minimum is narrow and shallow indicating that the SPP mode is significantly undercoupled to the incident radiation, in accordance with Eq. (5), i.e., $\Delta\omega_{rad}<\Delta\omega_{therm}$. As A_2 increases, $\Delta\omega_{rad}$ increases and the reflection minimum becomes deeper and wider. At $A_2\approx 5$ nm, maximum absorption occurs ($R_0\approx 0$), which indicates that at this amplitude $\Delta\omega_{rad}\approx\Delta\omega_{therm}$ is satisfied. As A_2 increases further, the mode becomes overcoupled to the free radiation and therefore the absorption minimum becomes even wider and shallower. From Fig. 3 we can also see that as A_2 increases the reflection minimum shifts slightly upwards in frequency due to the perturbation of the SPP mode by the long pitch component of the grating. In terms of perturbation

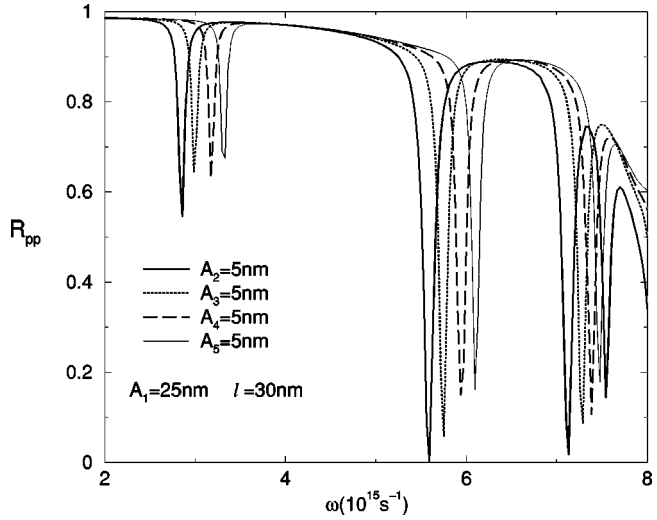

FIG. 4. Reflection coefficients for TM polarized normally incident radiation from four different double-period gratings, as defined by Eq. (1), with $n=2$, 3, 4, and 5, respectively. All these gratings have the same principal component ($A_1=25$ nm, $l=30$ nm), $A_n=5$ nm and $\alpha_n=0$.

theory, the frequency shift and the radiative broadening of the SPP mode are, respectively, associated with the real and imaginary parts of the self-energy of the SPP mode introduced by the weak long pitch component.

Until now we have considered only the case in which the double-period grating contains a principal short-period (l) Fourier component and a weak component with a period that is twice the principal one ($2l$). It is natural to ask what happens if we take $n>2$ in Eq. (1). In Fig. 4 we plot the reflection coefficients for TM polarized incident waves calculated for four different double-period gratings, as defined by Eq. (1), with $n=2$, 3, 4, and 5, respectively. In these calculations, we have taken $A_1=25$ nm, $l=30$ nm, $A_n=5$ nm, and $\alpha_n=0$. For the sake of clarity, in Fig. 4 we only plot the results in the frequency region $2\times10^{15}\ \mathrm{s}^{-1}<\omega<8\times10^{15}\ \mathrm{s}^{-1}$. (In the frequency region $\omega<2\times10^{15}\ \mathrm{s}^{-1}$, the incident radiation is almost totally reflected.) It can be seen that the reflection coefficient curves for the four double-period gratings are very similar. Each strong resonant absorption minimum corresponds to one band of the original sinusoidal grating with $A_1=25$ nm, and $l=30$ nm.

When a weak Fourier component with a period nl is added to the principal pure sinusoidal grating of period l, the size of the Brillouin zone is reduced by n times to $2\pi/nl$, and therefore each band of the original sinusoidal grating folds into n bands. Consequently, $I(n/2)$ values of k_x on each band of the original sinusoidal grating are folded to $k_x=0$ in the new Brillouin zone, where $I(n/2)$ is the integer part of $n/2$. In principle, all these SPP modes at $k_x=0$ can be excited by normally incident TM polarized radiation, thus each of these modes should lead to a resonance absorption. This expectation is clearly contrary to the results shown in Fig. 4. For example, in the case of $n=5$, two SPP modes ($k_x=2\pi/5l$, and $k_x=4\pi/5l$) in each band of the principal pure sinusoidal grating are folded to $k_x=0$, but only one resonant absorption minimum is seen in the frequency region of the original SPP band, as shown in Fig. 4. This apparent contradiction can be easily understood by considering the coupling strengths between the normally incident light and different SPP modes at $k_x=0$. It is most convenient to start from the SPP bands of the principal sinusoidal grating ($l=30$ nm) shown in Fig. 2(a). When the weak long-period (nl) component is introduced, it provides extra in-plane momenta ($k_x=m(2\pi/nl)$, where $m=1,2,3,\ldots$) for the photons, and therefore enables the direct coupling between normally incident photons ($k_x=0$) and the SPP modes with $k_x=m(2\pi/nl)$, which are the $k_x=0$ modes in the reduced Brillouin zone of the double-period grating. Since the weak long-period component is purely sinusoidal, the coupling between a $k_x=0$ photon and the $k_x=2\pi/nl$ SPP modes arises from first order perturbation, while coupling between a $k_x=0$ photon and a $k_x=m(2\pi/nl)$ SPP mode with $m>1$ corresponds to high order perturbation and therefore is much weaker. As a result, only the excitation of the $k_x=2\pi/nl$ mode on a SPP band of the principal sinusoidal grating can lead to strong absorption. This explanation is supported by comparing the frequencies of resonant absorption for the four double-period gratings shown in Fig. 4 with the SPP bands of the principal sinusoidal grating shown in Fig. 2(a). Because double-period gratings with different values of n probe slightly different parts of the dispersion curves of the principal sinusoidal grating, this provides an alternative approach for determining the SPP dispersion of the principal grating and for designing metal surfaces to give specific reflection properties.

IV. CONCLUSION

We study a zero-order double-period silver grating which consists of a principal sinusoidal component and a shallow long-period component. It is shown that, on a zero-order pure sinusoidal metal grating, the SPP modes within the light cone are strongly radiative and the absorption of normal incident TM polarized light is very weak except for the frequency region near $\omega_p/\sqrt{2}$. Outside the light cone, long range SPP modes are formed on a deep sinusoidal metal grating, but they can not be excited by incident radiation. In a double-period grating, the weak long-period component provides extra in-plane momenta for the incident photons and therefore allows the coupling between incident radiation and the long range SPP mode created by the principal deep grating. It is found that the excitation of these long range SPP modes leads to strong frequency selective absorption of incident radiation. The absorption frequencies and absorption lineshapes can be independently controlled by adjusting the amplitudes of the principal and the weak-long-period components of the grating, which promises many possible applications. This work also presents a simple example of designing the optical properties of metal surfaces by engineering the SPP band structures.

ACKNOWLEDGMENTS

The authors are grateful for the financial support provided by the Leverhulme Trust, the Biotechnology and Biological Science Research Council, and the Defense Evaluation Research Agency (Farnborough).

[1] H. Raether, *Surface Plasmons* (Springer-Verlag, Berlin, 1988); A. A. Maradudin, in *Surface Polaritons*, edited by V. M. Agranovich and D. L. Mills (North-Holland, New York, 1982), p. 405.
[2] B. Laks, D. L. Mills, and A. A. Maradudin, Phys. Rev. B **23**, 4965 (1981).
[3] W.-C. Tan, T. W. Preist, J. R. Sambles, and N. P. Wanstall, Acta. Photonica Sin. **27**, 91 (1998).
[4] M. B. Sobnack, W. C. Tan, N. P. Wanstall, T. W. Preist, and J. R. Sambles, Phys. Rev. Lett. **80**, 5667 (1998).
[5] W.-C. Tan, T. W. Preist, J. R. Sambles, and N. P. Wanstall, Phys. Rev. B **59**, 12 661 (1999).
[6] F. J. Garciá-Vidal and J. B. Pendry, Phys. Rev. Lett. **77**, 1163 (1996).
[7] J. Chandezon, M. T. Dupuis, G. Cornnet, and D. Maystre, J. Opt. Soc. Am. **72**, 839 (1982).
[8] L. Li, J. Opt. Soc. Am. A **11**, 2816 (1994).
[9] J. B. Harris, T. W. Preist, J. R. Sambles, R. N. Thorpe, and R. A. Watts, J. Opt. Soc. Am. A **13**, 2041 (1996).
[10] T. W. Preist, N. P. Cotter, and J. R. Sambles, J. Opt. Soc. Am. A **12**, 1740 (1995).
[11] G. Granet, Pure Appl. Opt. **4**, 777 (1995).
[12] N. P. Wanstall, T. W. Preist, W.-C. Tan, M. B. Sobnack, and J. R. Sambles, J. Opt. Soc. Am. A **15**, 2869 (1998).
[13] W. -C. Tan, T. W. Preist, J. R. Sambles, M. B. Sobnack, and N. P. Wanstall, J. Opt. Soc. Am. A **15**, 2365 (1998).
[14] D. J. Nash and J. R. Sambles, J. Mod. Opt. **43**, 81 (1996).
[15] F. Toigo, A. Marvin, V. Celli, and N. R. Hill, Phys. Rev. B **15**, 5618 (1975).
[16] G. Breit and E. P. Wigner, Phys. Rev. **49**, 519 (1936).